GLOBAL DESIGN OPTIMIZATION FOR FLUID MACHINERY APPLICATIONS

Wei Shyy (wss@aero.ufl.edu), Nilay Papila (nilay@aero.ufl.edu),
Kevin Tucker* (kevin.tucker@msfc.nasa.gov), Raj Vaidyanathan (raj@aero.ufl.edu),
and Lisa Griffin* (lisa.griffin@msfc.nasa.gov)

Department of Aerospace Engineering, Mechanics & Engineering Science
University of Florida, Gainesville, Florida 32611, USA

*NASA, Marshall Space Flight Center, AL 35812, USA

ABSTRACT

Recent experiences in utilizing the global optimization methodology, based on polynomial and neural network techniques, for fluid machinery design are summarized. Global optimization methods can utilize the information collected from various sources and by different tools. These methods offer multi-criterion optimization, handle the existence of multiple design points and trade-offs via insight into the entire design space, can easily perform tasks in parallel, and are often effective in filtering the noise intrinsic to numerical and experimental data. Another advantage is that these methods do not need to calculate the sensitivity of each design variable locally. However, a successful application of the global optimization method needs to address issues related to data requirements with an increase in the number of design variables, and methods for predicting the model performance. Examples of applications, selected from rocket propulsion components, including a supersonic turbine and an injector element, and a turbulent flow diffuser are used to illustrate the usefulness of the global optimization method.

1. INTRODUCTION & OVERVIEW

Modern computational and experimental fluid dynamics tools have matured to a stage where they can provide substantial insight into engineering processes involving fluid flows. This can help analyze the fluid physics as well as improve the design of practical devices. In particular, rapid and continuous development in the technology of fluid machinery demands that new design concepts be regularly proposed to meet goals for increased performance, robustness and safety while concurrently decreasing cost. These stringent goals are forcing consideration of design variables over ranges and in combinations not typically employed, thereby increasing the design complexity. Objective and efficient evaluation of these new and complex designs can be facilitated by development and implementation of systematic optimization methods. To date, the majority of the effort in design optimization of fluid dynamics has relied on gradient-based search algorithms (Baysal and Eleshaky 1992, Lambert et al. 1995, Reuther et al. 1999). These methods work iteratively through a sequence of local sub-problems, which approximate objective and constraint functions for a sub-region of the design space, e.g., by linearization using computed sensitivities. Major challenges for these optimization approaches are the robust and speedy computation of sensitivity coefficients (Elbanna and Carlson 1994, Dadone et al. 2000).

Polynomial-Based Response Surface

Recently we have witnessed increasing interests in utilizing the global optimization methods, which avoids the need to compute design sensitivities altogether. In this regard, the response surface methodology (RSM) has gained attention because minimum effort is required for software interfacing, which facilitates the integration of analysis and design codes. RSM is particularly suitable for subsystem approximation within multidisciplinary design optimization (Sobieszczanski-Sobieski and Haftka 1997) because it can utilize information collected from various sources and by different tools. It can also offer multi-criterion optimization, handle the existence of multiple design selections and related trade-offs, and address the noises intrinsic to numerical and experimental data. A main advantage of RSM lies in its robustness and intelligibility. Robustness and the smoothness of the approximations in noisy environments are achieved by performing extra analyses compared to the number of regression coefficients. This is a distinct advantage over derivative-based search algorithms, which may encounter difficulties in the presence of spurious local optima. This generality allows the consideration of information at varying levels of breadth (i.e., number of design variables) and depth (i.e., details of the design space). The significance of the individual design parameters can also be assessed directly by the global model. Another feature favoring RSM is its suitability for parallel computation.

The polynomial-based response surfaces are commonly employed in global optimization. An n^{th} order polynomial in each dependent variable is generated by standard least-squares regression (Myers and Montgomery 1995). Polynomial coefficients are obtained from a linear regression scheme. In addition to polynomials, neural networks (NN) can also be used to construct a response surface model. With a polynomial approach, there is a cost associated with RSM. The computational demands grow fast with increasing number of design variables, which is termed as the "*curse of dimensionality*". For example, to construct a second-order polynomial of N design variables, the number of coefficients to be fixed are $(N+1)(N+2)/(2!)$. A cubic model will require $(N+1)(N+2)(N+3)/(3!)$ coefficients. In

addition, the predictive capability of RSM is greatly influenced by the distribution of the sampling points in the design space (Unal et al. 1997, 1998).

Statistical techniques are also available for identifying polynomial coefficients that are not well characterized by the data. For example, a stepwise regression procedure based on t-statistics is often used to discard terms and improve the prediction accuracy. The t-statistic, or t-ratio, of a particular coefficient is given by the value of the coefficient divided by the standard error of the coefficient. The quality of fit of different surfaces can be evaluated by comparing the adjusted root mean square error, σ_a, defined as:

$$\sigma_a = \sqrt{\frac{\sum e_i^2}{n - n_p}} \qquad (1)$$

Here e_i is the error at i^{th} point of the training data, n is the number of training data points and n_p is the number of coefficients. The measure of error given by σ_a is normalized to account for the degrees of freedom in the model. Thus σ_a accounts for the nominal effect of higher order terms providing a better overall comparison among the different surface fits.

The accuracy of the models in representing the design space is further gauged by comparing the values of the objective function at test design points, different from those used to generate the fit, with the empirical solution. The root mean square error, σ, for the test set is given by:

$$\sigma = \sqrt{\frac{\sum \varepsilon_i^2}{m}} \qquad (2)$$

In this equation ε_i is the error at the i^{th} test point and m is the total number of test points.

Typically, the entire design data are divided into two groups. The major portion, called the training set, is used to fix the global model, and the minor portion, called the test set, is used to test the fidelity of the model. In short, the variation between the response surface (RS) and the training data, as given by Eq.(1), is normally used to judge the performance of the fit. As indicated in Eq. (2), additional test data can be employed to evaluate the performance of different polynomials over design points not used during the training phase.

In fluid dynamics applications, the RSM has been applied to a growing number of cases, including high speed civil transport (Knill et al. 1999), airfoil shape optimization (Rai and Madavan 1998, 2000, Madavan et al. 1999), diffuser shape optimization (Madsen et al. 2000), preliminary design of supersonic turbine, (Papila et al. 2000), and injectors (Shyy et al 1999, Tucker et al. 1998).

Data Selection in Design Space

In order to reduce the size of the data needed for constructing the global model, it is important to apply a sound strategy for selecting design points (Hafika et al. 1998). This strategy is referred to as the design of experiments. For example, face centered composite design (FCCD) is a popular approach for selecting the training data to aid the construction of a response surface model. In a three-dimensional space, FCCD creates a design space composed of eight corners of the cube, one at the center of each of the six faces and one at the center of the cube. Therefore, this yields (2^N+2N+1) points, where N is the number of design variables. Due to this scaling rule, FCCD is more effective when the number of design variables is modest, say, no larger than 5 or 6, but not a good choice for problems with large number of design variables.

The orthogonal array (OA) is a fractional factorial matrix that assures a balanced comparison of levels of any factor or interaction of factors. Because the points are not necessarily at vertices, the analytical tools can be more robust using the orthogonal array. The OA can significantly reduce the number of data required to construct a global model. To further reduce the data size, one can choose to rank the different point selections according to D-optimality criterion. This approach minimizes the generalized variance of the estimates, and can reduce the sensitivity of the response surface with respect to noise. In Papila et al. (2000), alternative representations of the design space are performed for supersonic rocket turbine design by using FCCD coupled with the D-Optimal treatment and OA. FCCD produces 77-data for the single-stage turbine with six design variables. With 11 design variables for the two-stage turbine design, FCCD yields 2,071-data. For three-stage turbine having 15 design variables, FCCD generates 32,799-data based on the formula of 2^N+2N+1, demonstrating the "*curse of dimensionality*". For such cases methods like OA can be applied to reduce the number of data in an efficient way.

To enhance the effectiveness of the RSM, as demonstrated by Papila et al. (2000), a multi-level approach is very useful. One can construct a global response surface and identify regions expected to be of favorable performance. Then, in these selected regions, one can refine the global model and identify the optimal design points with substantially higher accuracy.

Neural Networks

As already mentioned, NN techniques have also been used to generate surrogate models representing data obtained from simulations based on complex numerical and experimental schemes. Relevant papers by Carpenter & Barthelemy (1993), Nikolaidis et al. (1998), Greenman and Roth (1998), Madavan et al. (1998), Rai and Madavan (1998, 2000), Shyy et al. (1999), Papila et al. (1999) and Vaidyanathan et al. (2000) include comparative studies of polynomials and neural networks for data handling. NN is highly flexible in functional form and hence can offer significant potential for complex functions that cannot be adequately approximated by polynomials. NN can be effectively used in two ways. First, it can be used in conjunction with RSM. For example, in complex regions of the surface, NN can be trained using the existing data and then can be used to generate additional data thereby enhancing the available information in that particular area. Shyy et al. (1999) have demonstrated that this approach can help improve the fidelity of the polynomial-based response surface model. Alternatively, NN can generate data that can be directly used by the optimizer. With either a polynomial-based response surface method or a neural network method, the design optimization is conducted by first constructing a global representation of the design space, followed by a search for optimal designs.

While back-propagation neural networks (BPNN) have been largely employed in reported studies for NN-based design optimization, the radial-basis neural networks (RBNN) have

advantages that deserve to be investigated more closely. RBNN are multi-layer networks with hidden layers of radial basis transfer function and a linear output layer. The training of the network is a cyclic process and the weights and biases of the nodes of the network are adjusted until an accurate mapping is obtained. RBNN may require more neurons than BPNN, but they can be designed faster than the latter. Various parameters need to be evaluated to design an RBNN. For example, a *spread constant* is needed as a design parameter; i.e., the radius of the basis in the input space to which each neuron responds. One can design a network with zero error on the training vectors by generating as many radial basis neurons in the network as there are input vectors. A more compact design in terms of network size is obtained by generating one neuron at a time to minimize the number of neurons required. At each cycle/epoch, a neuron is added to the network until a user specified *error goal* is achieved or until the network has generated the maximum number of neurons possible. In such a case, an *error goal* and the *spread constant* need to be specified. The test data helps to evaluate the accuracy of the networks with varying spread constants. Thus, the test data are part of the evaluation process and help in selecting the best NN. The NN technique can encounter problems due to the nature of the data, as well as the construction of the neuron characteristics. If the training dataset is noisy, and the network is trained without proper filtering features, false optima due to over-fitting will occur. False optima can also be introduced when inadequate training data set is used.

In this paper, we summarize our recent experiences in utilizing the global optimization methodology related to polynomial-based RSM and NN. Then, we highlight three physical examples: a supersonic turbine and an injector element for rocket propulsion applications, and shape optimization of a turbulent flow diffuser. To reach a successful optimal design, one often needs to consider the issues related to (i) selection of appropriate representation of the design space for constructing the global model, (ii) employment of the statistical and testing tools to assess appropriate global models, (iii) multi-criterion optimization, (iv) existence of multiple design selections and related trade-offs, and (v) consideration of noises intrinsic to numerical and experimental data. There is no space to address all these matters in this paper, but detailed information can be found in the references cited.

2. PHYSICAL APPLICATIONS

Objective Functions

When attempting to optimize two or more different objective functions, conflicts between them arise because of the different relationships they have with the design variables. To solve this problem, a multi-objective approach is often employed. Here, competing objective functions are condensed to a single function by generating a composite objective function. The maximization of the composite function effectively optimizes the individual functions. The use of a response surface type of global model makes it straightforward to do such a multi-criterion optimization. Without response surfaces, it would have been a highly challenging task.

To handle such a multi-criterion optimization task, an average of some form is normally used to represent the composite function. For example, for the injector, the goal is to maximize the energy release efficiency, *ERE* while minimizing the chamber wall heat flux, Q. Shyy et al. (1999) and Tucker et al (1999) used a geometric mean to combine these two objectives and maximized the resulting composite objective function, D.

$$D = \left((d_{ERE})^s \cdot (d_Q)^t \right)^{1/2} \tag{3}$$

where the normalized function such as *ERE*, takes the form:

$$d_{ERE} = \left(\frac{ERE - A}{B - A} \right) \tag{4}$$

where B is the target value and A is the lowest acceptable value. Figure 1 illustrates the roles of s and t in the desirability function for the case of maximizing a response. The desirabilities with $s<<1$ imply that a product need not be close to the response target value, B, to be quite acceptable. However, a large value of s implies that the product is nearly unacceptable unless the response is close to B.

The other way of expressing the composite function is to use a weighted sum of the objective function. The composite desirability function can then be expressed as

$$D = \alpha_1 f_1 + \alpha_2 f_2 + \cdots \tag{5}$$

where D is the composite objective function and fs are the non-normalized objective functions. The αs are dimensional parameters that control the importance of each objective function. In the case of the supersonic turbine a weighted sum of the two objectives, the efficiency, η, and the weight, W, has been used. The expression, in the context of the turbine gives the incremental value of the payload, Δpay, with the change in W and η. The goal is to maximize Δpay, which in turn results in maximizing η and minimizing W and hence the payload is maximized.

$$D = \Delta pay = c_f(\eta - \eta_b) \times 100 - (W - W_b) \tag{6}$$

where η = the calculated efficiency
η_b = the baseline efficiency
W = calculated weight
W_b = the baseline weight
c_f = the amount of payload increment capacity for any efficiency gain

The baseline efficiency and weight are obtained with the existing design knowledge without benefiting from an optimization strategy. The goal of the optimization is to identify turbine configurations capable of delivering higher payload.

Turbulent Flow Diffuser

Figure 2 highlights the use of a response surface approximation for the optimum shape of a two-dimensional diffuser. The goal was to accomplish maximum pressure recovery by optimizing the wall contours. The flow is incompressible and fully turbulent with a Reynolds number of 10^5, based on the inlet throat half-width, D. The overall geometry is defined by the ratio of inlet and outlet areas, and the diffuser length to height ratio. In this study the length to height ratio is fixed at 3.0, and the area ratio at 2.0. The shape of the diffuser wall is designed for

optimum performance, with five design variables represented by B-splines. The CFD model is based on the full Reynolds-averaged Navier-Stokes equations, with the k-ε two-equation turbulence model in closure form. At the inlet of the flow domain, a uniform flow distribution is specified. Detailed discussion of this study can be found in Madsen et al. (2000). As illustrated in Fig. 1, within the fidelity of the analysis tool, there are often multiple design points that meet the design objectives. It is interesting to note that different diffuser shapes are found to yield essentially the same performance. The response surface model is ideally suitable for such situations.

Supersonic Turbine

Next, we summarize our recent efforts in optimizing the preliminary design of a supersonic turbine suitable for a *reusable launching vehicle* (RLV) propulsion system. Single-, two- and three-stage turbines are considered with the number of design variables increasing in accordance with the number of stages. There are 2 types of design variables:

Geometric input

- mean diameter (D)
- last rotor annulus area (A_{annl})
- blade height ratio between the 1st vane and the last rotor blade
- vane and blade axial chords

Performance Variables

- RPM
- number of stages
- blade row reaction
- work split (if more than 1 stage is investigated)

In the work presented by Papila et al. (2000), there are 6, 11, and 15 design variables for the single-, two- and three-stage turbines, respectively. In addition, there are 2 structural constraints, the blade centrifugal stress and the disk stress. The blade centrifugal stress was constrained by a limit placed on the product of the blade exit annulus area and the RPM^2/A^2_{annl}. The disk stress was constrained by a limit placed on the pitchline velocity (the product of the RPM and the mean radius). All the design variables involved in the design process are normalized by their respective baseline values.

For rocket engine applications, maximizing the vehicle payload for a given turbine operating condition is the ultimate objective. Any gain in turbine efficiency will be reflected in a reduced propellant consumption, thus an increase in payload. However, higher turbine performance usually entails multistage designs, which are heavier. To ascertain required predictive capability of the RSM, a two-level domain refinement approach has been adopted in the course of optimization (Papila et al. 2000). First, a response surface was constructed for the entire design space. Since the accuracy of the response surface was less than satisfactory, a domain refinement was then adopted based on the initial optimization.

An inspection of the optimal designs indicates that the two-stage turbine gives the best payload performance for this application. As the number of the stage increases, we see that efficiency improves while the weight increases also. According to the formula for Δpay, the improvement in efficiency from two- to three-stage cannot compensate the penalty from higher weight. As shown in Figure 3, the mean diameter, speed, and the exit blade area exhibit distinct trends. Specifically, the diameter decreases, speed increases, and annulus area decreases with increasing number of stages. It is interesting to observe that none of the selected values of the design parameters are toward the limiting values assigned, indicating that the optimal designs result from compromises between competing parametric trends. For such cases, a formal optimizer such as the present response surface method is very useful. The results indicate that the efficiency rises quickly from single stage to two stages but the increase is much less pronounced with three stages. A single-stage turbine performs poorly under the engine balance boundary condition possibly due to a significant portion of fluid kinetic energy being lost at the turbine discharge of the single-stage design due to high stage pressure ratio and the high-energy of the working fluid, which is predominantly hydrogen. Figure 4 summarizes fitting/training and testing results of RBNN and polynomial-based approximations for Δpay of a 2-stage turbine. The training data are selected based on the orthogonal array approach. There are 11 design variables, 249 training data (OA), and 78 testing data in both original and refined design spaces. Centered on the optimal design point predicted using the information gathered for the entire design space, the reduced design space has 20% of the range originally assigned to each design variable. In all plots, a perfect fit will result in a 45-degree line.

The effectiveness of the multi-level RSM approach can be observed in this figure by comparing the original and refined design space plots. While RBNN is obviously more accurate for the training data due to more number of adjustable parameters associated with the number of neurons, its predicting capability, as reflected in the testing data plots, may not be as superior. Nevertheless, RBNN is attractive because it has the flexibility to handle complex characteristics of a response surface and is straightforward to train because the computation is based on the linear regression analysis.

Swirl Coaxial Injector Element

The injector considered is for the combustor of an advanced liquid rocket engine. Different injector concepts have been proposed for this purpose, including shear coaxial type, impinging type, and swirl type (Shyy et al. 1999, Tucker et al. 1999). The swirl coaxial element has been used somewhat sparingly in the U.S.A., but has been widely used in Russia because of its reported ability to perform well over a large throttle range (Gill and Nurick 1976). Figure 5 shows that the GO_2, flowing in the center post of the element, exits from the element with both radial and axial velocity components. This effect is achieved by introducing the GO_2 tangentially into the center post through small slots. The empirical design methodology of Calhoon et al. (1973) uses the oxidizer pressure drop, ΔP_o, fuel pressure drop, ΔP_f, combustor length, L_{combl}, and the full cone swirl angle, Θ, as independent variables. Due to stability considerations for this injector design, the ΔP_o range is set to 10-20% of the chamber pressure, while the ΔP_f range is set to 2-20% of chamber pressure. The combustor length, defined as the distance from the injector to the end of the barrel portion of the chamber ranges from 2-8 inches. The full cone swirl angle is allowed to vary from 30-90°. The dependent variables modeled are ERE (energy release efficiency, a measure of element

performance), wall heat flux, Q_w, injector heat flux, Q_{inj}, relative combustor weight, W_{rel}, and relative injector cost, C_{rel}.

With the multi-criterion optimization, one can assess the effect of certain aspects of the design during the optimization process. The set of results shown in Table 1 facilitate the illustration. The baseline results in Table 1 are obtained by placing equal weight for all design variables. Alternatively, in Case 1, we place more emphasis on reducing the wall and injector face heat fluxes. Desirability functions for both of these variables are given increased weights (5 and 10, respectively). Since lower heat fluxes tend to increase component life, weighting these two variables is equivalent to emphasizing a life-type issue in the design. Since Q_w is already at its minimum value, it remains fixed. As expected, Θ is decreased which decreases the value of Q_{inj} by almost 35%. The lower value of Θ also produces a lower *ERE*. Both propellant pressure drops and the combustor length are increased to mitigate the drop in *ERE*. The increases in L_{comb} and ΔP_j cause an increase in W_{rel} and C_{rel}, respectively. The emphasis on life extracts the expected penalty on performance. Additionally, for the current model, there are also slight weight and cost penalties.

The results for Case 2 are obtained by emphasizing maximization of *ERE* and minimization of W_{rel} with desirability weightings of 10 and 5, respectively. Increased weighting for these two variables is equivalent to emphasizing a thrust to weight goal for the injector/chamber. The relative chamber length is shortened to slightly lower W_{rel}. *ERE* is maximized by increasing the GO_2 swirl angle by a factor of almost 2.5 and increasing ΔP_j by over 35 %. The value of *ERE* increases by over one percent. As noted earlier, increasing Θ leads to increased injector heat flux. For this case, emphasis on thrust and weight tends to have an adverse affect on Q_{inj}. Relative cost, C_{rel}, for the current model, is also increased significantly. Figure 6 offers a visual illustration of the trends exhibited in various scenarios between a swirl type and an impinging type injector. While the qualitative features between the two injectors are consistent, the present optimization model allows the inspection of the parametric variations directly.

3. CONCLUSIONS

The global optimization method can be particularly effective with either a polynomial-based response surface or a neural network when information from different computational, experimental, and analytical sources needs to be assembled. In this paper, we summarize our recent experiences in utilizing the optimization methodology for optimizing tasks related to the preliminary design of a supersonic turbine, the design of an injector element, and the shape optimization of a turbulent flow diffuser. A successful optimal design often needs to address the issues related to the selection of appropriate training data for constructing the global model, employment of the statistical and testing tools to identify appropriate global models, multi-criterion optimization, existence of multiple design selections and related trade-offs, and consideration of noises intrinsic to numerical and experimental data.

4. ACKNOWLEDGMENTS

The work presented has been supported by NASA Marshall Space Flight Center. The paper is a summary of our collaboration with our colleagues, as cited in the references given below.

5. REFERENCES

Baysal, O. and Eleshaky, M.E., 1992 "Aerodynamic Design Optimization Using Sensitivity Analysis and CFD", *AIAA Journal* Vol.30 pp.718-725.

Calhoon, D., Ito, J. and Kors, D., 1973 "Investigation of Gaseous Propellant Combustion and Associated Injector-Chamber Design Guidelines," Aerojet Liquid Rocket Company, *NASA CR-121234, Contract NAS3-13379.*

Carpenter, W.C. and Barthelemy, J.-F.M, 1993 "A comparison of Polynomial Approximations and Artificial Neural Nets as Response Surface," *Structural Optimization*, Vol. 5, pp. 166-174.

Dadone, A., Valorani, M. and Grossman, B., 2000 "Smoothed Sensitivity Equation Method for Fluid Dynamic Design Problems," *AIAA Journal*, Vol. 38, pp. 418-426.

Elbanna, H.M. and Carlson, L.A., 1994 "Aerodynamic Sensitivity Coefficients Using the Three-Dimensional Full Potential Equations", J. Aircraft Vol.31, pp.1071-1077.

Gill, G. S., and Nurick, W. H., 1976 *Liquid Rocket Engine Injectors*, NASA SP-8089.

Greenman, R. M. and Roth, K.R., 1998 "High-Lift Optimization Design Using Neural Network," Proceedings of DETC98, *ASME Computers in Engineering Conference*, Atlanta, Georgia, DETC98/CIE-6006.

Greenman, R. M. and Roth, K.R., 1999 "Minimizing Computational Data Requirements For Multi-Element Airfoils Using Neural Networks," *37th AIAA Aerospace Sciences Meeting and Exhibit*, Reno, Nevada, AIAA 99-0258.

Haftka, R.T., Scott, E.P. and Cruz, J.R., 1998 "Optimization and Experiments: A Survey," *Applied Mechanics Review*, Vol. 51, pp. 435-448.

Knill, D.L., Giunta, A.A., Baker, C.A., Grossman, B., Mason, W.H., Haftka, R.T. and Watson, L.T., 1999 "Response Surface Models Combining Linear and Euler Aerodynamics for Supersonic Transport Design," *Journal of Aircraft*, Vol. 36, pp. 75-86.

Lambert, P.A., Lecordix, J.L., and Braibant, V. 1995 "Constrained Optimization of Nacelle Shapes in Euler Flow using Semi-analytical Sensitivity Analysis" *Structural Optimization*, Vol.10, pp.239-246.

Madavan, N.K, Rai, M.M. and Huber, F. W., 1999 "Neural Net-Based Redesign of Transonic Turbines for Improved Unsteady Aerodynamic Performance," *AIAA/SAE/ASME/ASEE 35th Joint Propulsion Conference*, AIAA 99-2522.

Madsen, J.I., Shyy, W. and Haftka, R.T. 2000 "*Response Surface Techniques for Diffuser Shape Optimization*," accepted for publication in *AIAA Journal*.

Myers, R.H. and Montgomery, D.C., 1995 *Response Surface Methodology* (Pro-cess and Product Optimization Using Designed Experiments), Wiley, New York.

Nikolaidis, E., Long, L., and Ling, Q., 1998 "Neural Networks and Response Surface Polynomials for Design of Vehicle Joints," *39th AIAA/ASME/ASCE/AHS/ASC Structures, Structural Dynamics, and Materials Conference*, Long Beach, California, AIAA-98-1777.

Papila, N., Shyy, W., Fitz-Coy, N. and Haftka, R.T., 1999 "Assessment of Neural Net and Polynomial-Based

Techniques for Aerodynamic Applications," 17th Applied Aerodynamics Conference, Norfolk, VA, AIAA 99-3167.

Papila, N., Shyy, W., Griffin, L., Huber, F. and Tran, K., 2000 "Preliminary Design Optimization for a Supersonic Turbine for Rocket Propulsion," *AIAA/SAE/ASME/ASEE 35th Joint Propulsion Conference*, Paper No. 2000-3242.

Rai, M.M. and Madavan, N.K, 1998 "Aerodynamic Design Using Neural Networks," *7th AIAA/USAF/NASA/ISSMO Symposium on Multidisciplinary Analysis and Optimization*, St. Louis, AIAA 98-4928.

Rai, M.M. and Madavan, N.K, 2000 "Improving the Unsteady Aerodynamic Performance of Transonic Turbines Using Neural Networks," *38th AIAA Aerospace Sciences Meeting and Exhibit*, Reno, Nevada, AIAA 2000-0169.

Reuther, J., Alonso, J.J., Rimlinger, M.J. and Jameson, A., 1999 "Aerodynamic Shape Optimization of Supersonic Aircraft Configurations via an Adjoint Formulation on Distributed Memory Parallel Computers," *Computers and Fluids*, Vol. 28, pp. 675-700.

Shyy, W., Tucker, P.K. and Vaidyanathan, R., 1999 "Response Surface and Neural Network Techniques for Rocket Engine Injector Optimization," *AIAA/SAE/ASME/ASEE 35th Joint Propulsion Conference*, AIAA 99-2455.

Sobieszczanski-Sobieski, J. and Haftka, R.T., 1997 "Multidisciplinary aerospace design optimization: survey of recent developments", *Structural Optimization*, Vol. 14, pp.1-23.

Tucker, P.K., Shyy, W. and Sloan, J.G., 1998 "An Integrated Design/Optimization Methodology for Rocket Engine Injectors," *AIAA/SAE/ASME/ASEE 34th Joint Propulsion Conference*, AIAA-98-3513.

Tucker, P. K., Shyy, W. and Vaidyanathan, R., 1999 "Optimization of a GO_2/GH_2 Impinging Injector Element," *NASA 10th Thermal and Fluids Analysis Workshop*, September 13-17, Huntsville, AL.

Tucker, P. K., Shyy, W. and Vaidyanathan, R., 1999 "Optimization of a GO_2/GH_2 Swirl Coaxial Injector Element," *Penn State University Propulsion Engineering Research Center 11th Annual Symposium on Propulsion*, November (1999).

Unal, R., Braun, R. D., Moore, A.A., and Lepsch, R.A., 1997 "Response Surface Model Building Using Orthogonal Arrays for Computer Experiments," *19th Annual International Conference of the International Society of Parametric Analysis*, New Orleans, Louisiana.

Unal, R., Lepsch, R. A., and McMillin, M. L., 1998 "Response Surface Model Building and Multidisciplinary Optimization using D-Optimal Designs," *7th AIAA/USAF/NASA/ISSMO Symposium on Multidisciplinary Analysis and Optimization*, Paper No. 98-4759.

Vaidyanathan, R., Papila, N., Shyy, W., Tucker, P.K., Griffin, L. W., Haftka, R.T. and Fitz-Coy, N., "Neural Network-Based and Response Surface-Based Optimization Strategies for Rocket Engine Component Design," *8th AIAA/USAF/NASA/ISSMO Symposium on Multidisciplinary Analysis and Optimization*, Paper No. 2000-4880.

Table 1. Effect of emphasizing life and performance issues on optimal injector design.

Independent Variable	Constraints	Results Baseline	Constraints	Results Case 1	Constraints	Results Case 2
DP_o	100-200	104	100-200	200	100-200	200
DP_f	20-200	20	20-200	32	20-200	44
L_{comb}	2-8	3.4	2-8	3.6	2-8	2.9
Q	30-90	44.0	30-90	30.0	30-90	72.0
Dependent Variable	*Baselin* Variable Weight		*Emphasis on Life*		*Emphasis onThrust to Weight*	
ERE	1	95.7	1	95.3	10	96.7
Q_w	1	0.596	5	0.596	1	0.596
Q_{inj}	1	10.5	10	6.9	1	22.6
W_{rel}	1	0.98	1	0.99	2	0.96
C_{rel}	1	0.76	1	0.79	1	0.94

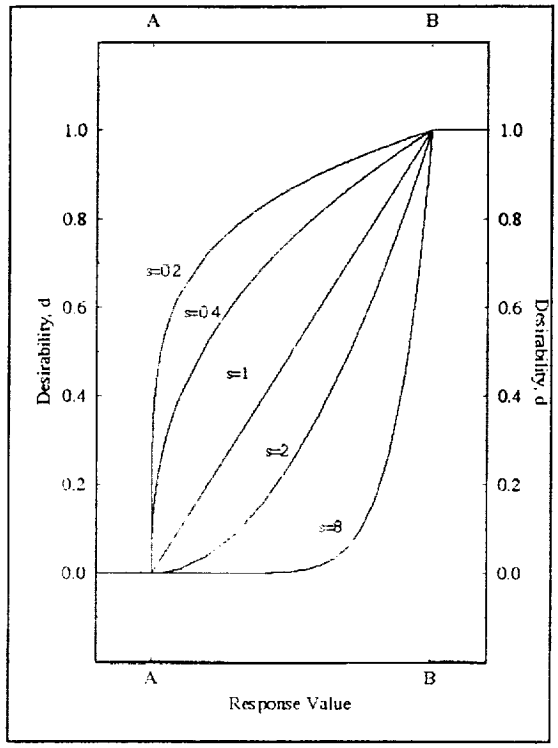

Figure 1. Desirability function for various weight factors, *s*.

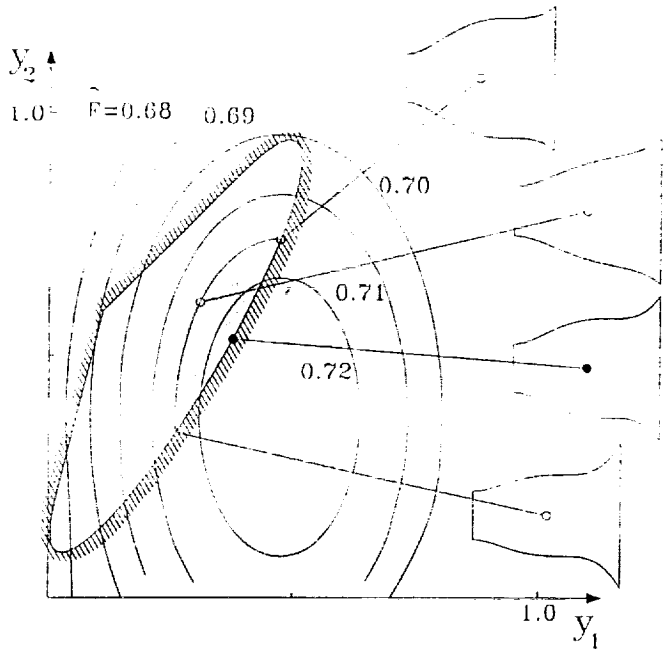

Figure 2. Contour plot of response surface for diffuser design. Solid circle indicates the optimal region. The hatched part of the feasible space comprises designs with performance within 1% of the optimal. Corresponding shapes are indicated to the right. The results indicate that multiple design points meet the goal.

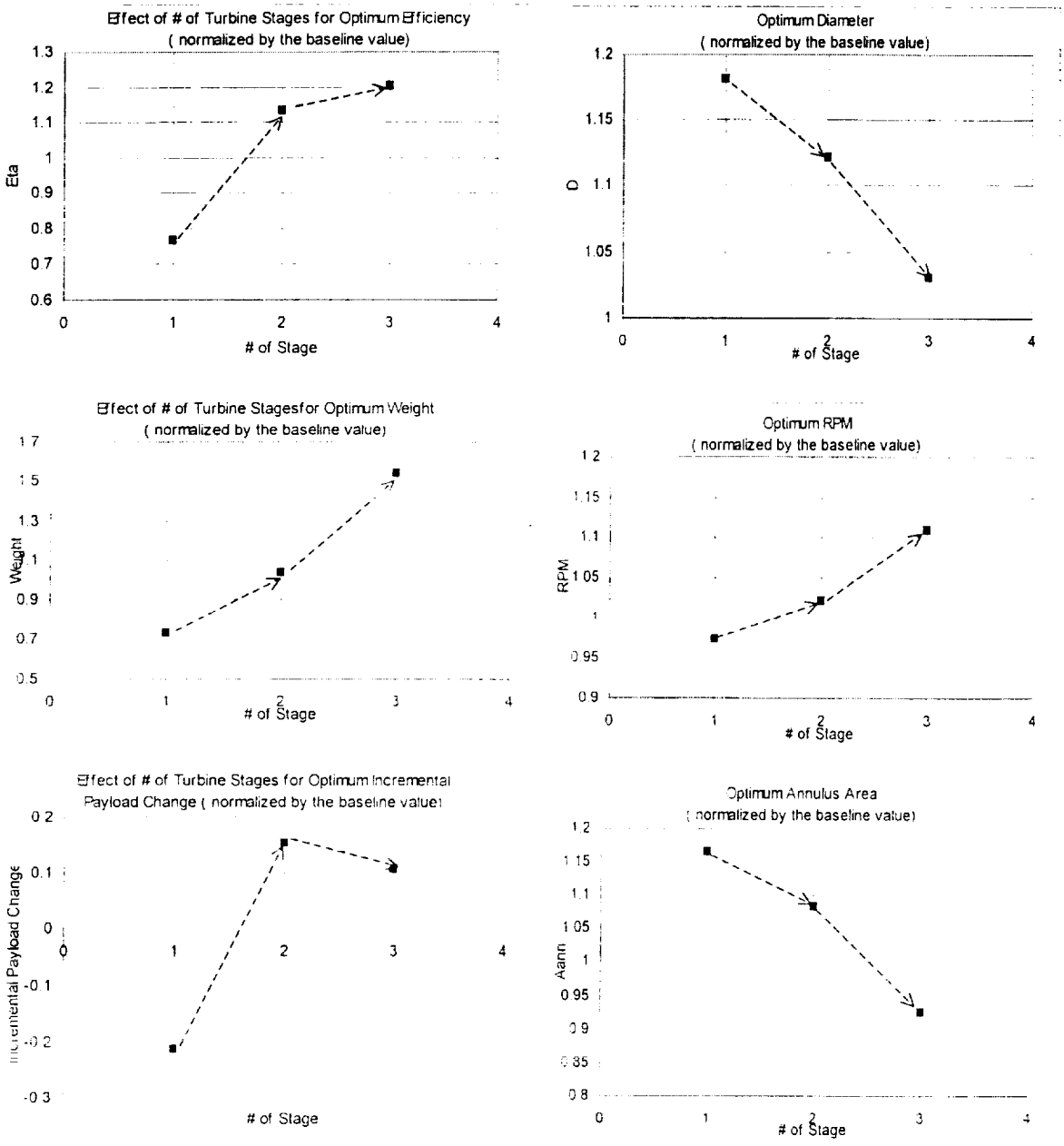

Figure 3. Effect of the number of turbine stage on optimum output parameters; η, W, and Δpay and optimum design parameters; D, RPM, and A_{ann} calculated for Δpay-based optimization. All design variables are normalized by the baseline values.

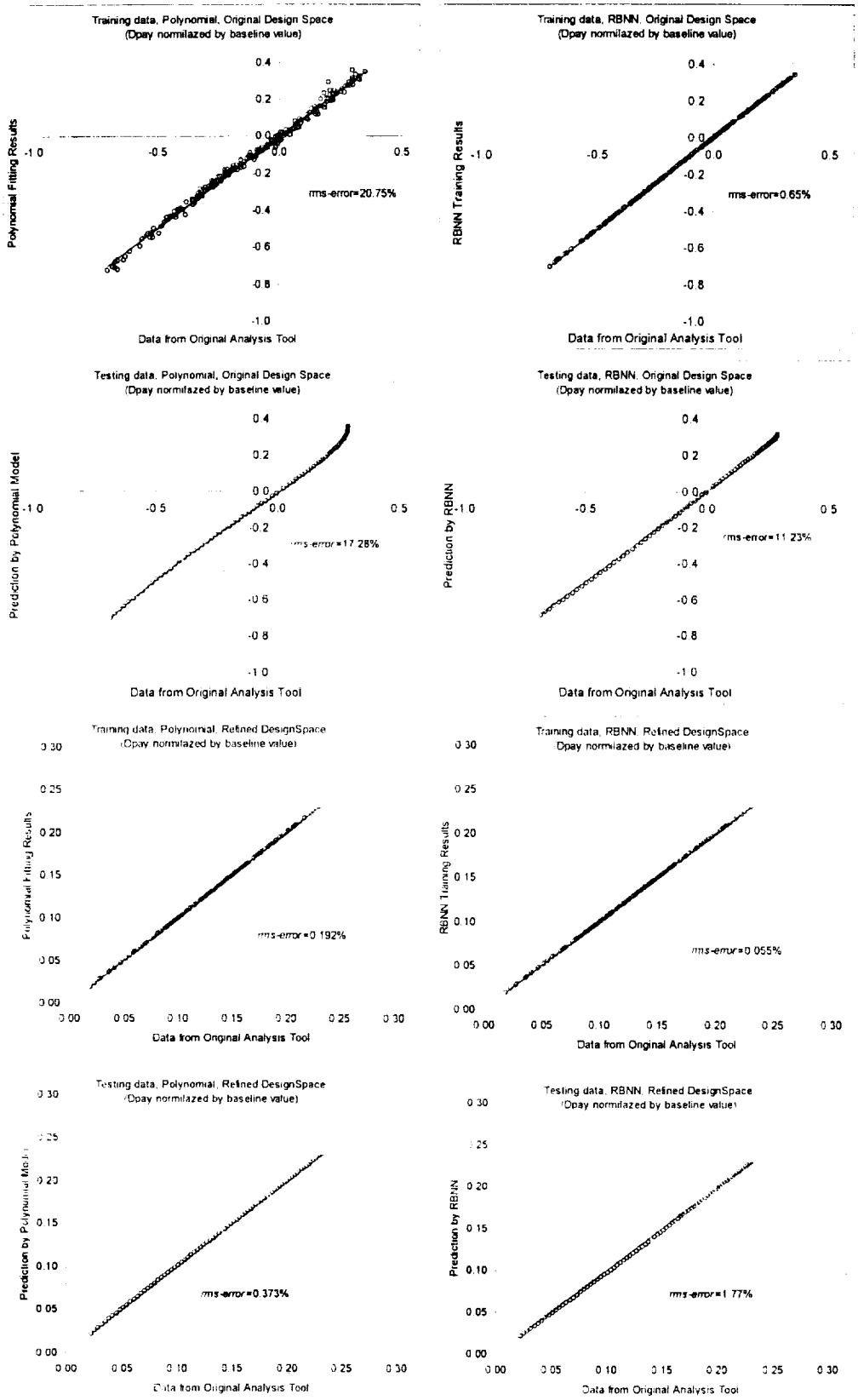

Figure 4. Comparison of NN and polynomial-based representations for 2-stage supersonic turbine. Plotted are the original and predicted values of Δpay. A perfect fit will result in a 45-degree line. The training and testing data are selected based on the orthogonal arrays with the D-optimal criterion. There are 11 design variables, 249 training data (OA), and 78 testing data in both original and refined design spaces. (The values for Δpay are normalized by the baseline value)

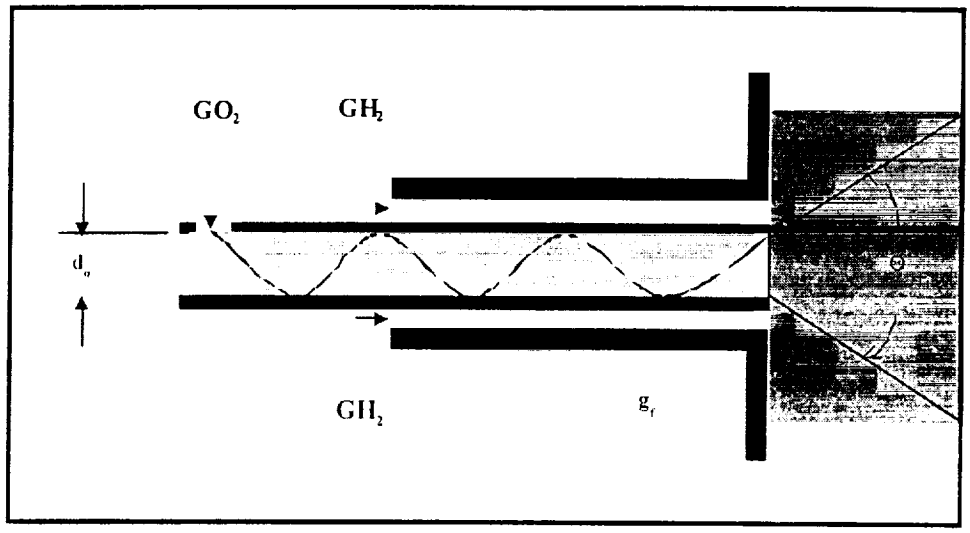

Figure 5. Swirl coaxial injector element schematic

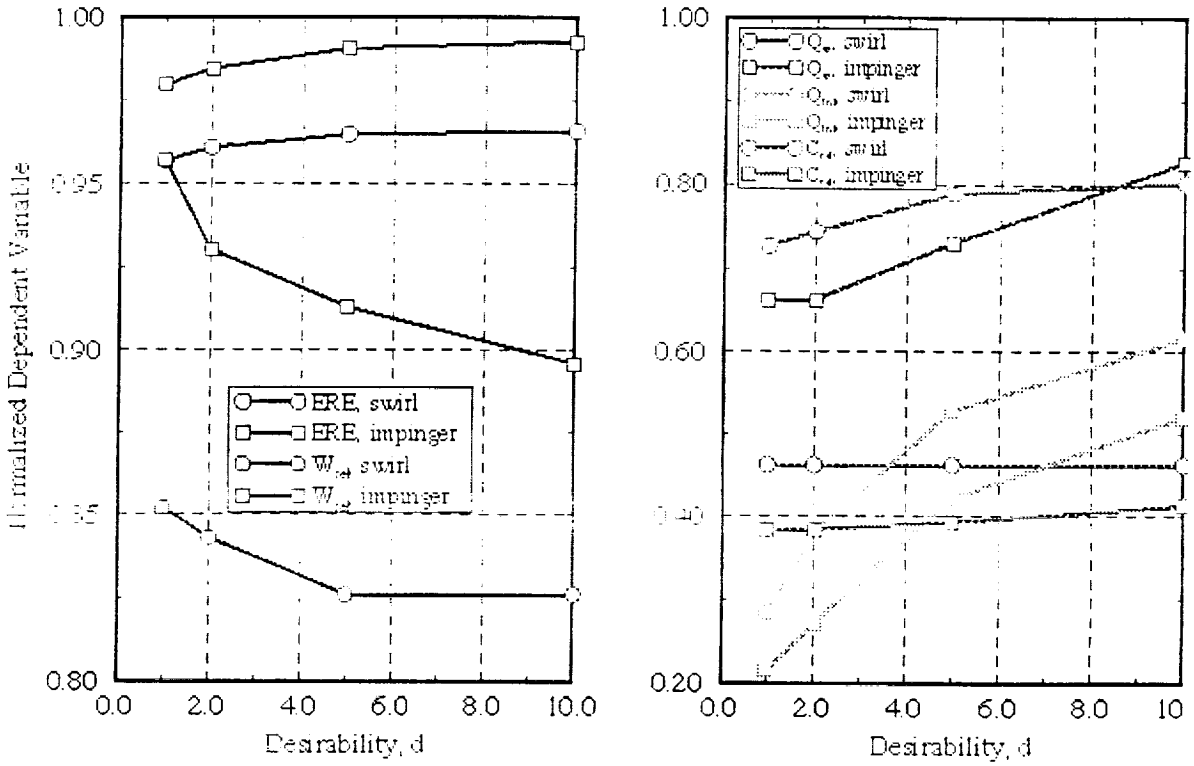

Figure 6. Thrust to Weight Trends for Swirl and Impinging Elements